BMC Microbiology

RESEARCH

Open Access

Genome-to-function integrated exploration of polyethylene biodegradation by *Rhodococcus opacus* R7

Jessica Zampolli[1], Mattia Salvadori[1], Valentina Vincenti[1], Marina Lasagni[2] and Patrizia Di Gennaro[1*]

Abstract

Background Polyethylene (PE) is the most widely produced polyolefin and represents a major contributor to plastic waste, largely due to its chemical stability and resistance to biological degradation.

PE biodegradation is typically characterized as a series of oxidative metabolic processes rather than mineralization. An urgent priority is the development of integrated experimental setups that bring together physiological, biochemical, and molecular analyses under controlled cultivation conditions to unlock the metabolic traits of PE biodegradation.

This study aims to elucidate the molecular mechanisms of commercial low-molecular-weight PE (LDPE) attack by *Rhodococcus opacus* R7 through an integrated genome-to-function approach, including growth and extracellular laccase assays, intracellular lipid quantification, gas chromatography coupled with mass spectrometry (GC–MS) analysis of compounds associated with untreated LDPE, and transcriptional profiling of oxidative enzymes.

Results LDPE utilization was evaluated under multiple cultivation strategies (1% single-dose vs. 0.4% fed-batch), inoculum conditions, and polymer types (untreated or UV-pretreated) over 28 days.

Fed-batch LDPE (0.4%) supported slightly higher viable cell numbers than fixed-dose LDPE (1%), while prolonged PE pre-adaptation did not enhance growth. Extracellular laccase activity was detected under all conditions, but was more influenced by the physiological status of the inoculum than by PE concentration or pretreatment. Lipid accumulation was early detected in case of 1% PE, while the fed-batch conditions reflected the growth phase and physiological responses. GC–MS analyses revealed that LDPE oxidation products vary compared to abiotic and control samples. Specifically, fixed-dose LDPE favored a progressive change in the pattern-profile of carboxylic acids and medium- to long-chain alkanes, while fed-batch LDPE produced a heterogeneous mixture, including alcohols and ketones, consistent with a continuous and asynchronous transformation of the polymer.

The fed-batch condition induced a broader and earlier transcriptional activation of oxidative genes, including seven laccase-like multicopper oxidases (*LMCOs*), alkane monooxygenase (*alkB*), benzoate dioxygenase (*benA*), and cytochrome P450 hydroxylase. Long-chain *n*-alkanes, particularly tetracosane (C24), strongly induced oxidative enzymes, suggesting their role as metabolic signals during PE degradation.

*Correspondence:
Patrizia Di Gennaro
patrizia.digennaro@unimib.it

Full list of author information is available at the end of the article

© The Author(s) 2026. **Open Access** This article is licensed under a Creative Commons Attribution-NonCommercial-NoDerivatives 4.0 International License, which permits any non-commercial use, sharing, distribution and reproduction in any medium or format, as long as you give appropriate credit to the original author(s) and the source, provide a link to the Creative Commons licence, and indicate if you modified the licensed material. You do not have permission under this licence to share adapted material derived from this article or parts of it. The images or other third party material in this article are included in the article's Creative Commons licence, unless indicated otherwise in a credit line to the material. If material is not included in the article's Creative Commons licence and your intended use is not permitted by statutory regulation or exceeds the permitted use, you will need to obtain permission directly from the copyright holder. To view a copy of this licence, visit http://creativecommons.org/licenses/by-nc-nd/4.0/.

Conclusions Overall, LDPE attack by *R. opacus* R7 emerges as a dynamic process shaped by substrate accessibility and cultivation strategy, highlighting its potential as a platform for controlled plastic biodegradation.

Keywords Actinobacteria, Low-density polyethylene, Lipid accumulation, Laccase activity, Oxidase and oxygenase expression

Introduction

Polyethylene (PE), a semi-crystalline polyolefin, is the most manufactured synthetic polymer with a global production exceeding 150 million tonnes in 2023 [1, 2]. Depending on molecular weight and degree of branching, PE is mainly classified in low-density polyethylene (LDPE) and high-density polyethylene (HDPE) [3, 4]. The polymer is mainly composed of aliphatic C-H and C–C bonds which contribute to its chemical inertness and strong resistance to degradation. Consequently, PE remains in the environment playing a significant role in the global accumulation of plastic waste. Its recycling remains limited and incomplete due to established technological and economic constraints [5].

Chemical and biological catalysis have emerged as promising approaches to improve plastics recycling. Biocatalysts generally operate under mild conditions, making them energy-efficient tools for polymer break down and/or upcycling [6, 7]. Moreover, an increasing number of newly isolated microorganisms have been reported to exhibit the ability to oxidize or biodegrade PE [8–10]. Early investigations to assess microbial metabolic potential on PE predominantly employed model compounds, such as medium- and long-chain *n*-alkanes [11, 12]. Alkanes act as metabolic inducers of diverse genes and correspondent enzymatic systems such as oxidoreductases (monooxygenases, hydroxylases, oxidases), esterases, proteases, hydrolases in both fungi (e.g., *Fusarium, Aspergillus*) and bacteria (e.g., *Acinetobacter, Pseudomonas, Alcanivorax, Rhodococcus*) [12–16]. Beyond enzymatic potential, efficient PE transformation requires microbial colonization of hydrophobic polymer surfaces [17].

In recent years, increasing attention has been devoted to the role of abiotic pretreatments (UV, thermal, or oxidative) in modulating PE susceptibility to microbial attack, although their effectiveness and impact on subsequent biological processes remain debated [18]. Moreover, emerging evidence suggests that PE transformation is not driven by single enzymes, but rather involves the coordinated action of multiple oxidative and catabolic systems, including multicopper oxidases, monooxygenases, and downstream β-oxidation pathways.

Within this conceptual framework, both fungal and bacterial taxa genera are gaining prominence as PE degraders [19], with key bacterial genera including *Streptococcus*, *Klebsiella*, *Acinetobacter*, *Bacillus*, *Ralstonia*, *Stenotrophomonas*, *Comamonas*, *Delftia*, *Pseudomonas*, and *Rhodococcus* [8, 10]. Members of *Rhodococcus* genus have attracted particular interest due to their metabolic versatility and capacity of degrading diverse plastic polymers [9, 20, 21] (Additional file 1- Table S1). For instance, *R. ruber* strain C208 achieves 8% weight reduction of UV-pretreated PE in one month and a mineralization rate of up to 1.2% yr^{-1} through the activation of alkane and fatty acid β-oxidation pathways [22–24]; *R. erythropolis* D4 increases in cell number in a few days (7 days) and metabolizes PE as sole carbon and energy source showing laccase-like activity [8]; *Rhodococcus* sp. A34 is able to reduce PE weight by 1% in 30 days and activates multiple extracellular proteins in a short range of time [25]. Similarly, *R. opacus* strain R7 exhibits remarkable metabolic versatility towards plastic polymers including polyesters and polyolefins [26, 27]. Specifically, *R. opacus* R7 showed a rapid growth on PE used as the sole carbon and energy source. Building on our previous transcriptomic and biochemical characterization of *R. opacus* R7 grown on polyethylene [26, 28], which revealed the early induction of oxidative enzymes (alkane monooxygenase, and a cytochrome P450 hydroxylase), membrane transporters, as well as three extracellular laccase-like multicopper oxidases (*LMCO1*, *LMCO2*, and *LMCO3*), several key aspects of PE biodegradation remain unresolved. *R. opacus* R7 also grows efficiently on medium- and long-chain *n*-alkanes [29], suggesting a potential link between hydrocarbon metabolism and PE degradation. However, whether alkanes can modulate or enhance PE-degrading pathways in R7 is unknown. In particular, the regulation of oxidoreductases, the influence of cultivation strategies, and the contribution of inducers remain unresolved. Therefore, R7 represents a promising model to test whether different growth conditions and hydrocarbon inducers can enhance PE degradation, a feature potentially exploitable for plastic valorisation.

Although considerable progress has been made in the study of microbial plastic degradation, PE mineralization is still largely proposed and under debate, since it is thought as a transformation process composed of oxidative and metabolic steps [9, 30]. A substantial fraction of the available evidence relies on exploratory or predictive approaches, including genomic inference and indirect physio-chemical analyses of the polymer and its putative degradation products [31]. Simultaneously, attention has shifted from depolymerization alone towards the selective formation of value-added intermediates, highlighting the biotechnological potential of PE transformation

beyond waste removal. Together, these considerations underline the need for combined experimental configurations that integrate physiological, biochemical and molecular analyses under controlled cultivation conditions to better resolve the metabolic basis and outcomes of PE biodegradation.

The present study aims to elucidate the molecular basis of PE attack by *Rhodococcus opacus* R7 through an integrated genome-to-function approach. To achieve this goal, PE utilization by *R. opacus* R7 was investigated under different cultivation strategies (LDPE added as 1% single-dose *vs*. 0.4% fed-batch or the effect of pre-cultivation on LDPE) and two types of LDPE (untreated or UV-pretreated) up to one month of incubation. The laccase activity as the main extracellular activity in relation to PE oxidation, and the intracellular lipid accumulation were assessed as physiological and biochemical parameters; LDPE attack was also monitored by metabolite production analyses. These outcomes were related to the transcriptional responses of candidate oxidases and oxygenase obtained under these conditions, thereby linking genomic potential to functional metabolic activity. Furthermore, the influence of potential molecules acting as inducers was investigated to promote PE biodegradation.

Material and methods

Chemicals

The polyethylene powder used in this work was supplied from Merck Life Science (Mn = 1700 by GPC, Mw = 4000 by GPC, code 427,772, Merk Life Science S.r.l., Italy) and is reported as commercial low-molecular-weight PE (LDPE).

LDPE was sterilized for 1 h under UV using a 15 W UV-C germicidal lamp λ ~ 220–240 nm (Gelaire Flow Laboratories, Italy).

LDPE was pre-treated by a QUV chamber (Q-LAB Corporation, USA) using the following alternate ageing cycle: 8 h at 60 °C (no humidity), with UV-A at 340 nm (0.76 W/m^2) and 4 h at 50 °C with 100% humidity, and no light for a total of 42 days.

Bacterial strain and growth conditions

R. opacus strain R7 (CIP identification number 107348, deposited to the Institute Pasteur Collection) was isolated from polycyclic aromatic hydrocarbon contaminated soil and it is regularly cultivated in M9 mineral medium (M9) [32] added with 20 mM malate (M9-M) for up to 24 h.

A previous work demonstrated the ability of *R. opacus* R7 to grow in the presence of PE as the only carbon and energy source up to 7 days [26].

Based on these data, in the present work diverse growth conditions were evaluated. First, the preliminary inoculum was obtained after R7 cells were washed twice from overnight malate culture by centrifuging at 8500 rpm (5804 R, Eppendorf, Italy) and inoculated in a fresh M9 mineral medium supplemented with sterilized LDPE powder at 1% (M9-PE), as the only carbon and energy source. The absence of malate was verified by incubating R7 cell deriving from M9-M culture in no-carbon inoculum. The M9-PE pre-culture was incubated up to 72 h. Two different growth conditions were assessed from M9-PE pre-cultures: (i) M9 added with 1% sterile PE powder (M9-PE1%), (ii), M9 supplemented with 0.4% sterile PE powder at 0, 3, 7, 14, and 21 days (M9-PE0.4%), directly to the ongoing culture. At each time, an additional 0.4% w/v sterile PE powder was added directly to the ongoing culture. Starting from malate pre-culture, the same conditions were applied, obtaining (iii) M9-PE1%-preM and (iv) M9-PE0.4%-preM conditions, and (v) M9 supplemented with 0.4% sterile UV pre-treated PE powder at 0, 3, 7, 14, and 21 days (M9-UV-PE0.4%), following the same fed-batch supplementation procedure described above. These conditions were designed to compare different PE availability regimes rather than to isolate the feeding schedule as a single independent variable. Specifically, M9-PE1% represented a single initial PE exposure, whereas M9-PE0.4% and M9-UV-PE0.4% represented repeated PE supplementation conditions intended to evaluate the response of R7 to progressive PE availability during incubation.

R7 inoculum was established in 100 mL- or 250 mL-flasks with 1:5 of medium at 0.1 initial cell optical density (OD) measured at 600 nm (OD_{600}) and incubated at 30 °C under shaking (120 rpm) for up to 28 days.

R7 cell growth was determined at 0, 3, 7, 14, 21, and 28 days by OD_{600} measurements and with the colony-forming unit counting method by serially diluting 0.1 mL of bacterial cultures in a solution of M9 mineral medium and plating on Luria–Bertani (LB) agar medium. For viable cell count, cultures were vigorously shaken and vortexed before sampling to resuspend PE particles and detach PE-associated cells as much as possible. Aliquots used for serial dilution and plating therefore contained a mixed fraction of suspended cells and PE-associated cells detached during sample homogenization. Plates were incubated at 30 °C for 48 h. Both OD_{600} and CFU ml^{-1} data are reported as the mean of three biological replicates with standard deviation (SD).

To verify the absence of growth supported by residual malate, washed R7 cells derived from malate-grown cultures were inoculated into M9 medium without any added carbon source. This no-carbon control was processed under the same incubation conditions used for PE-containing cultures.

Moreover, a previous study demonstrated the ability of *R. opacus* R7 to biodegrade medium- and long-chain *n*-alkanes [29]. Therefore, we exploited this ability to

evaluate if these substrates can enhance PE biodegradative activities. Indeed, R7 strain was also grown on potential intermediates of PE degradation such as long-chain *n*-alkanes with 24, or 36 carbon atoms (0.1% C_{24} or 0.8% C_{36}, respectively) (Merck Life Science S.r.l., Italy). The growth assays were established in 50 mL flasks from $OD_{600} \sim 0.1$ and the growth was measured by the optical density up to 72 h for C_{24} or 14 days for C_{36}.

Enzymatic activity

Enzymatic activity was monitored measuring extracellular laccase activity for all assessed growth conditions as indicator of initial PE oxidative activity. At specific sampling times (0, 3 7, and 14 days), *R. opacus* R7 cultures were harvested for 10 min by centrifugation at 9000 rpm (Eppendorf, Italy) to collect the supernatant that was filtrated to remove the residual LDPE using 0.45 µm filters (Millipore, Italy). The resulting cell-free supernatant (CFS) was lyophilized and resuspended in 50 mM potassium phosphate buffer pH 7 (PPB) in a twenty-fifth of the initial volume.

Laccase enzymatic activity was determined in 50 mM potassium phosphate buffer (pH 7) using 30 mM 2,6-dimethoxyphenol (2,6-DMP) at 470 nm (ε: 14.8 mM^{-1} cm^{-1}) by adding 100 µM $CuSO_4$ in 1 cm-cuvettes and analyzed by UV–visible spectrophotometer (Ultraspec 2100 *pro*, Amersham Biosciences) as described in [26].

The hydrolytic activity of CFS from *R. opacus* R7 grown on M9-UV-PE0.4% was assessed as follows. The lyophilized CFS obtained as described above was resuspended in 1/40 of the initial volume of 10 mM PPB. The hydrolytic activity of concentrated CFS was tested in the presence of 20 mM *p*-nitrophenyl acetate (*p*NPA; Merck Life Science, Italy) dissolved in isopropanol in 1 ml final volume of 10 mM Tris–HCl pH 8, 1% TritonX-100 at 25 ∘C.

One unit (U) of enzyme activity is defined as the amount of enzyme catalyzing the formation of 1 µmol of *p*-nitrophenol per minute under the reported conditions. Hydrolytic specific activity was defined as the amount of protein required to hydrolyze 1 mM *p*NPA under the assay conditions by increasing absorbance at 405 nm during 5-min intervals, for up to 30 min. The measure of the enzymatic activity was carried out by a UV/visible spectrophotometer (Ultraspec 2100 pro, Amersham Biosciences).

The total protein concentration of the lyophilized CFS was assessed using BCA Protein Assay Kit (Merck Life Science, Italy). Protein concentrations were calculated from the bovine serum albumin standard curve.

Blank reactions, used for background subtraction, contained all reaction components at the same concentrations but without CFS. The abiotic controls (no CFS) were incubated for each time point, lyophilized, resuspended, concentrated, and assayed under the same conditions as the biological samples. The enzymatic activity was calculated as U mL^{-1} and reported as the mean of three replicates ± standard error (SE).

Quantification of lipid accumulation and fluorescence microscopy

Intracellular lipid accumulation in *R. opacus* R7 was evaluated using complementary qualitative and quantitative approaches. Quantitative determination of total intracellular lipids was performed using the sulfophosphovanillin (SPV) colorimetric assay [33]. Briefly, cell pellets obtained from 9 mL of each culture were resuspended in 40 µL of minimal medium and mixed with 360 µL of concentrated sulfuric acid (95–98%, v/v) in glass tubes. Samples were heated at 100 °C for 10 min, cooled to room temperature, and reacted with 1 mL of phosphovanillin reagent, followed by incubation at 37 °C for 15 min. After 45 min of color development in the dark, absorbance was measured at 530 nm using a UV–visible spectrophotometer. Lipid concentrations were calculated from a calibration curve prepared with oleic acid standards supplemented with a defined amount of *R. opacus* R7 cells and expressed as mg of lipids per CFU of R7 culture.

For fluorescence microscopy, *R. opacus* R7 cells (10 µL) collected at different kinetic times were mixed with 4',6-diamidino-2-phenylindole (DAPI) (1.5 µL; stock 1 mg mL^{-1} in dimethyl sulfoxide) and Nile Red (2 µL; stock 1 mg mL^{-1} in dimethyl sulfoxide, diluted 1:5 before use, Sigma-Aldrich, St. Louis, MO, USA) and placed on a glass slide. DAPI was used to visualize cellular DNA (excitation 355 nm, emission 465 nm), while Nile Red selectively stained neutral lipid inclusions, emitting in the red–orange range depending on lipid polarity (excitation 488 nm, emission 520–590 nm). Samples were covered with a coverslip, incubated in the dark to prevent photobleaching, and observed using a Thunder fluorescence microscope (LEICA Microsystem, Italy) equipped with a 100 × oil-immersion objective (Camera DFC9000 GTC, Leica, Italy). Images were acquired using the DFT5101X filter cube, with Nile Red fluorescence set to approximately 12% intensity, allowing qualitative evaluation of lipid droplet distribution and relative abundance.

The lipid concentration was obtained from two biological replicates.

GC–MS product analyses deriving from LDPE attack by *R. opacus* R7

LDPE attack was evaluated on M9-PE1%-preM or M9-PE-feed0.4%-preM cultures by GC–MS analyses. M9-PE flasks without inoculum were used as the abiotic controls which were processed identically as the inoculated samples at every time point. Cell-only controls, extraction blanks, and solvent blanks were also processed

and analyzed in parallel with the samples. Malate-grown control consisted of *R. opacus* R7 cultures on M9-M (malate 20 mM) incubated and processed under the same conditions, whereas extraction blanks and solvent blanks were used to monitor background signals potentially derived from solvents, glassware, derivatization reagents, or sample preparation. Peaks detected in blank chromatograms or malate-grown control were considered background contaminants or cell-associated/background metabolic profile and were not interpreted as PE-associated transformation products.

The detected products were recorded for up to 28 days (0, 14, and 28 days) by extracting the metabolic products from bacterial cultures with half a volume of dichloromethane (DCM) by manually shaking the separation funnel for 10 min and repeating the extraction twice. The samples were derivatized as reported in [27] before injecting 1 µL in a 6890 N Network gas chromatograph (GC) system (J&W DB-5 ms 60 m × 0.25 mm, 0.25 µm Ultra Inert GC Column, Agilent Technologies, Santa Clara, CA, USA) with He at 99.99% as a carrier gas, coupled to a 5973 Network Mass Selective Detector (MSD, Agilent Technologies) at 70 eV in full scan mode (40–600 Da). The instrument was set as described in Zampolli et al. [28]. MSD ChemStation E.02.02.1431 (Agilent Technologies, Santa Clara, CA, USA) was used to analyze the resulting chromatograms. Unknown compounds were putatively annotated by comparison with the NIST11 mass spectral database. Library matches showing similarity scores ≥ 90% were retained. The detected products under each condition were then grouped into chemical classes. Peak areas were normalized, and the relative abundance of each compound class was calculated as the ratio of the individual compound peak area to the total peak area, multiplied by 100 [28]. All the experiments were carried out in duplicate.

Analyses for genetic trait prediction of *R. opacus* R7 genome in silico

The prediction of genes potentially involved in PE oxidation in *R. opacus* R7 was based on previous transcriptomic data [26] and literature evidence on PE metabolism. Genome annotation and functional prediction were performed using the Rapid Annotation using Subsystem Technology (RAST) server [34] and NCBI Prokaryotic Genome Annotation pipeline [35]. The predicted gene products were aligned by the Clustal Omega program multiple sequence alignment (MSA) tool [36] with the default settings.

The resulting laccase-like multicopper oxidases (aa LMCOs sequences) were evaluated for the presence of amino acid translocation signal using SignalP (v. 6.0) [37] to predict their potential ability to be secreted extracellularly. Specifically, the tools enable the prediction of secretory signal peptides transported by the Sec translocon and cleaved by Signal Peptidase I (Lep) (Sec/SPI), lipoprotein signal peptides transported by the Sec translocon and cleaved by Signal Peptidase II (Lsp) (Sec/SPII), Tat signal peptides transported by the Tat translocon and cleaved by Signal Peptidase I (Lep) (Tat/SPI), Tat lipoprotein signal peptides transported by the Tat translocon and cleaved by Signal Peptidase II (Lsp), (Tat/SPII), or Pilin and pilin-like signal peptides transported by the Sec translocon and cleaved by Signal Peptidase III (PilD/PibD) (Sec/SPIII). Only LMCOs presenting a translocation signal were selected.

Moreover, selected LMCOs (aa sequences) were compared with the amino acid sequences of LMCOs/laccases previously associated with PE oxidation or polymer oxidation, as well as with well-characterized bacterial and fungal laccases, using MSA tool of Clustal Omega with default parameters [36]. The comparison included the laccases from *Trametes versicolor* (PDB ID: 1KYA), *Bacillus subtilis* (PDB ID: 3ZDW), a reference multicopper oxidase (PDB ID: 3GDC), Lac15 from a marine microbial metagenome (PDB ID: 4F7K), and the LMCO from *Rhodococcus ruber* C208 (C208) [22].

Nucleic acid extraction and manipulation

Total RNA was isolated from up to 100 mL *R. opacus* R7 cells grown on M9-PE1%-preM, M9-PE0.4%-preM at different time points or 20 mL cells grown on M9-M at exponential growth phase by using RNA Power Soil Total RNA Isolation Kit (Qiagen Italia, Italy) according to the manufacturers' procedure with slight modifications [26]. Finally, the extracted RNA was dissolved in 50 µL of RNase-free water. RNA concentration and purity were evaluated spectrophotometrically with a NanoDrop OneC Spectrophotometer based on A260/280 and A260/230 ratios (Thermo Fisher Scientific, Italy). RNA integrity was assessed qualitatively by 0.8% agarose gel electrophoresis based on the electrophoretic profiles (Bio-Rad, Italy).

Quantitative real-time PCR (RT-qPCR)

The transcriptional induction of the *R. opacus* R7 genes potentially encoding enzymes involved in PE degradation was evaluated by quantitative reverse transcription (RT-) qPCR experiments [15].

The considered growth conditions include M9-PE1%-preM, M9-PE0.4%-preM, and malate which was used as a reference in order to determine the relative abundance of target transcripts. The amplified genes encode laccase-like multicopper oxidases (*LMCO1*, *LMCO2*, *LMCO3*, *LMCO4*, *LMCO5*, *LMCO6*, *LMCO7*), a 1-alkane monooxygenase (*alkB*), a cytochrome P450 hydroxylase (*P450II*), and a benzoate dioxygenase (*benA*), and 16S rRNA. The gene expression was evaluated by the ΔΔCt

method, and normalized using the 16S rRNA gene as a reference. The reverse transcription of the total RNA was performed with iScriptcDNA Synthesis kit (BIO-RAD, Italy) to obtain 200 ng cDNA with the following thermocycling conditions: 5 min at 25 °C followed by 1 h at 42 °C and then 5 min at 85 °C. The amplification of the cDNA obtained was carried out using the StepOnePlus Real-Time PCR System (Applied Biosystem, Italy) in 10-µL qPCR volume containing 4.4 µL of the reverse-transcribed RNA samples, 5 µL of PowerUp SYBR Green Master Mix (Applied Biosystem, Thermo Scientific, Italy), and 300 nM of each primer listed in Additional file 2—Table S2. The temperature program was set as follows: 30 s at 95 °C, followed by 40 cycles of 5 s at 95 °C, 10 s at 60 °C and 45 s at 72 °C and one cycle of 15 s at 95 °C, 1 min at 60 °C and 15 s at 60 °C. Primer specificity was confirmed by melting-curve analysis, which showed a single amplification peak for each primer pair. Amplification efficiencies were determined for each primer pair using standard curves generated from serial dilutions of cDNA. Amplification efficiencies ranged from 93% to 98%, with standard-curve R^2 values of 0.99. In order to exclude DNA contamination, no-reverse-transcriptase controls were performed by omitting the reverse transcriptase in RT-PCR experiments, which were conducted with the same temperature program and primer sets for 35 cycles of amplification. No amplification was detected in these controls.

Relative gene expression was calculated using the $2^{-\Delta\Delta Ct}$ method, with 16S rRNA as the reference gene and malate-grown cells as the reference condition. Data are expressed as mean ± standard deviation derived from at least three independent experiments and three technical replicates.

Statistical analysis

Bacterial growth, laccase activity, and lipid data were assessed by two-way repeated-measures ANOVA using a linear mixed-effects model, with sample, time, and their interaction as fixed effects, and biological replicate as a random effect. Post-hoc pairwise comparisons were performed using estimated marginal means with Tukey adjustment for multiple comparisons. Significance levels are indicated as follows: p-value < 0.05 (*), < 0.01 (**), < 0.001 (***), or < 0.0001 (****).

Results

Growth kinetic of *Rhodococcus opacus* R7 on LDPE

The ability of *R. opacus* R7 to utilize PE as the sole source of carbon and energy was previously demonstrated, with peak growth reached within three days (2×10^8 CFU mL^{-1}) with a cell increase of almost two orders of magnitude, which was stable up to 7 days [26].

In this study, *R. opacus* R7 was tested for various growth conditions in the presence of LDPE in a long-term degradation assay until 28 days. Figure 1 and Additional file 3—Figure S1 show the growth of R7 cultivated in M9-PE1%, M9-PE0.4%, M9-PE1%-preM, M9-PE0.4%-preM, or M9-UV-PE0.4%.

Considering the viable cells, R7 achieved the maximum cell growth at 28 days in M9-PE0.4% and M9-PE0.4%-preM conditions equal to $4.25 \pm 0.75 \times 10^8$ CFU mL^{-1} and 4.6 ± 0.6 10^8 CFU mL^{-1}, respectively. The highest increase in cell numbers was of two orders of magnitude for R7 grown on M9-PE0.4%-preM. In addition, OD_{600} showed

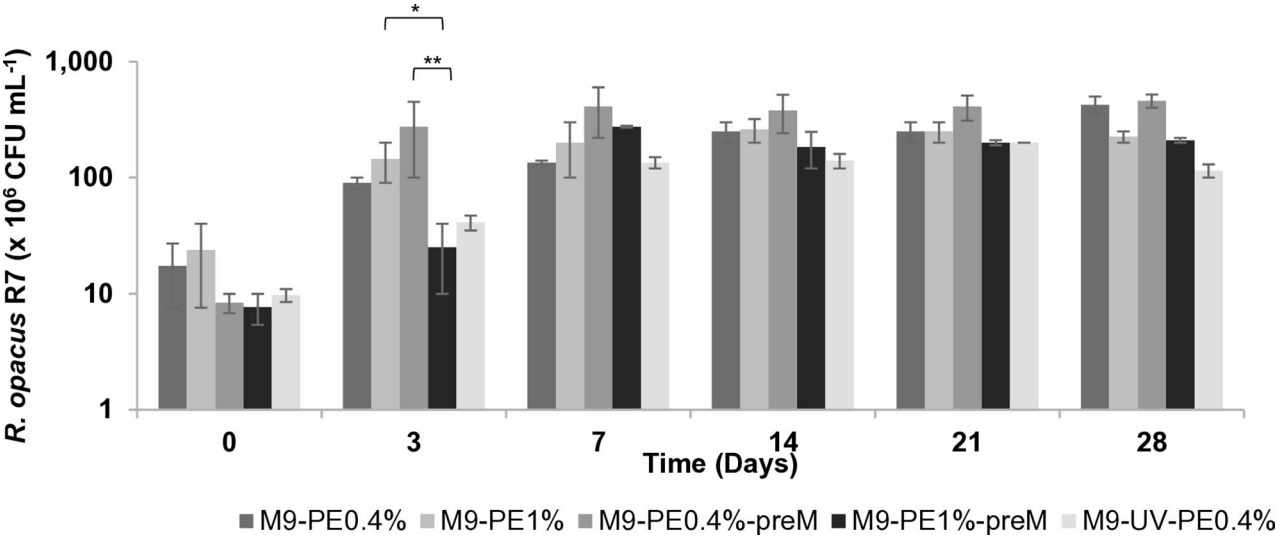


Fig. 1 Growth of *R. opacus* R7 on different conditions recorded at 0, 3, 7, 14, 21, and 28 days. The growth is presented as the mean value of the viable cell counts of *R. opacus* R7 (CFU $mL.^{-1}$) ± St. Dev. The Y-axis is shown on a logarithmic scale. The statistical significance was calculated by ANOVA followed by Tukey-adjusted post-hoc comparisons: p-value < 0.05 (*), p-value < 0.01 (**)

the maximum growth for M9-UV-PE0.4%, as well as M9-PE0.4% and M9-PE0.4%-preM conditions, accounting respectively for OD_{600} equal to 0.80 ± 0.03, 0.9 ± 0.3, and 0.68 ± 0.03 (Additional file 3—Figure S1). This discrepancy between the two measures is due to the optical contribution of PE particles and their fragmentation in suspension, as well as to cell aggregation and adhesion to the polymer surface, which can lead to an overestimation of turbidity and an underestimation of viable cell counts.

Moreover, statistical analysis showed a significant main effect of sample (*p-value* < 0.05), and a highly significant main effect of time (*p-value* < 0.0001), while the sample × time interaction was not significant. Tukey-adjusted post-hoc comparisons were then performed between samples at each time point showing significant differences mainly at 3 days: M9-PE0.4%-preM was significantly different with respect to M9-PE1%-preM (*p-value* < 0.05), and M9-PE1% was significantly different from M9-PE1%-preM (*p-value* < 0.05).

Overall, these results indicate that the M9-PE0.4%-preM condition promotes *R. opacus* R7 growth, as reflected by the biomass increase over time, instead of an excessively prolonged pre-adaptation phase on the polymer, which may reduce cell viability, likely inducing metabolic stress and impairing the ability to colonize PE.

Screening of enzymatic activity during growth of *Rhodococcus opacus* R7 on LDPE

The extracellular laccase activity was assessed after *R. opacus* R7 growth under different PE-conditions as indication of initial PE-degrading activity. The enzymatic assay was performed using 2,6-DMP as one of the typical substrates for laccase activity and in the presence of $CuSO_4$, since copper is known to be an enhancer of laccase activity [22, 28].

Based on the growth results of *R. opacus* R7 in the presence of LDPE under different experimental settings (M9-PE1%, M9-PE0.4%, M9-PE1%-preM, M9-PE0.4%-preM, or M9-UV-PE0.4%), extracellular enzymatic assays were performed on the cell-free supernatants (CFS) to assess laccase activity. Increasing evidence suggests that they contribute to the oxidation of polyolefins by promoting the formation of reactive sites along the PE chain. Previous studies have demonstrated that laccase-like multicopper oxidases secreted by *R. opacus* R7 play a key role in the initial phase of LDPE oxidation in the extracellular environment [26, 28]. Therefore, evaluating their activity is central to understanding the mechanisms underlying the observed polymer degradation.

These analyses were aimed at monitoring PE metabolism during the early kinetic phases of growth, up to 14 days (sampling times 3, 7, and 14 days).

Relative laccase activity of M9-PE1%-preM, M9-PE0.4%-preM, or M9-UV-PE0.4% conditions showed higher laccase catalysis during the entire incubation period, compared to M9-PE1%, M9-PE 0.4% conditions, although they were within the same order of magnitude (Fig. 2).

At day 3, laccase activity reached respectively $(3.6 \pm 0.9) \times 10^{-2}$ U mL^{-1}, $(3.3 \pm 0.5) \times 10^{-2}$ U mL^{-1}, and $(2.4 \pm 0.3) \times 10^{-2}$ U mL^{-1} in the M9-PE1%-preM, M9-PE0.4%-preM, M9-UV-PE0.4% conditions, compared to 1.2×10^{-2} U mL^{-1} and $(2 \pm 1) \times 10^{-2}$ U mL^{-1} in M9-PE1%, M9-PE0.4% conditions, respectively. While laccase activity remained relatively constant up to 14 days in these two last conditions, as well as for M9-UV-PE0.4%, it progressively increased in M9-PE1%-preM

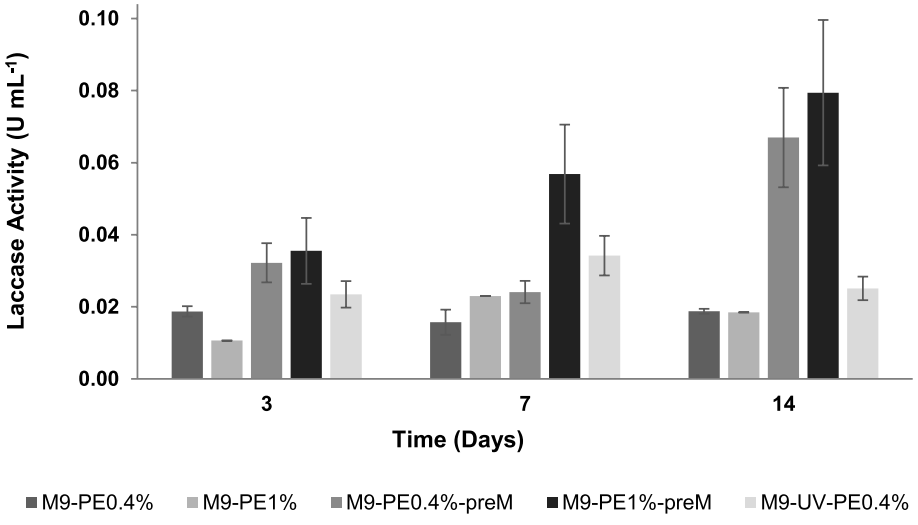


Fig. 2 Laccase activity (U mL^{-1}) in the supernatants (CFS) of *R. opacus* R7. Laccase activity was measured using 2,6-dimethoxyphenol (2,6-DMP) as a substrate after growth under the different PE-supplementation conditions. $CuSO_4$ was added at a final concentration of 100 µM during the enzymatic assay. Data are reported as the mean of three replicates ± SE

and M9-PE0.4%-preM cultures, reaching $(8.0 \pm 2) \times 10^{-2}$ U mL^{-1} and $(7 \pm 1) \times 10^{-2}$ U mL^{-1}, respectively. This trend is consistent with the growth data and supports the assumption that pre-cultivation on malate enhances the metabolic activity of *R. opacus* R7, promoting a stronger extracellular enzymatic response (Fig. 1). However, no significant differences in laccase activity profiles were observed between the two PE concentrations (PE 1% vs PE 0.4% in fed-batch), as both conditions showed comparable trends over time, suggesting that PE concentration and feeding strategy do not significantly affect extracellular laccase activity.

Notably, during cultivation on M9-UV-PE0.4%, no increase in laccase activity was observed during the early stages of cultivation, despite previously detected improved growth and cell viability. This apparent discrepancy suggests that enhanced substrate accessibility primarily supports metabolic processes other than laccase induction, such as the direct utilization of pre-oxidized or low-molecular-weight fractions. Based on literature evidence, other enzymatic activities can occur, such as lipase or hydrolase activity [25]. In addition, UV-PE is a different substrate than untreated PE, more hydrophilic, presenting unsaturation in carbon chain or ester bonds. Therefore, the extracellular lipase activity was assessed on the CFS of *R. opacus* R7 grown on UV-pretreated PE (M9-UV-PE0.4%) at different time points (3, 7, 14, and 21 days) to evaluate the subsequent step of PE-degrading activity. The enzymatic assay was performed spectrophotometrically using *p*NPA as a substrate for lipase activity [28]. Interestingly, the extracellular lipase activity was observed at early times of growth (3 and 7 days) with values of 0.02 ± 0.01 and 0.04 ± 0.02 (Additional file 4—Figure S2). At further sampling times, the extracellular activity decreases, due to an internalization of oligomers or oxidized products which can be processed by other enzymatic systems [26]. The evaluation on UV-PE condition preliminarily suggests that other enzymatic systems than laccases initiate the biodegradative process of per-oxidized PE, in particular an extracellular activity was evident.

In general, the extracellular laccase activity represents a specific component of *R. opacus* R7 metabolism, influenced mainly by the initial physiological state of the cells rather than by PE concentration or pre-treatment. Based on these results, subsequent analysis will be focused on the utmost conditions: M9-PE1%-preM, M9-PE0.4%-preM, or M9-UV-PE0.4%.

Quantification of lipid accumulation and fluorescence microscopy observation of *Rhodococcus opacus* R7 cells grown on LDPE

To assess whether lipid accumulation contributed to the metabolic slowdown of *R. opacus* R7 during growth on M9-PE1%-preM, M9-PE0.4%-preM, or M9-UV-PE0.4% conditions, total intracellular lipids were evaluated using a SPV spectrophotometric assay and by fluorescence microscopy at different cultivation times (3, 7, 14, 21, and 28 days).

Quantitative SPV assays revealed different levels and trends of intracellular lipid accumulation for the diverse growth conditions (Fig. 3).

In the cultures grown on M9-PE1%-preM, the highest lipid content was detected at 3 days and it decreased at 7 days up to 28 days. While cultures grown with fed-batch PE supplied at 0.4% showed a more gradual and stable trend of cell-associated lipid accumulation over time. Statistical analysis showed a significant effect of growth conditions, incubation time and temporal patterns of lipid accumulation that differed among the tested

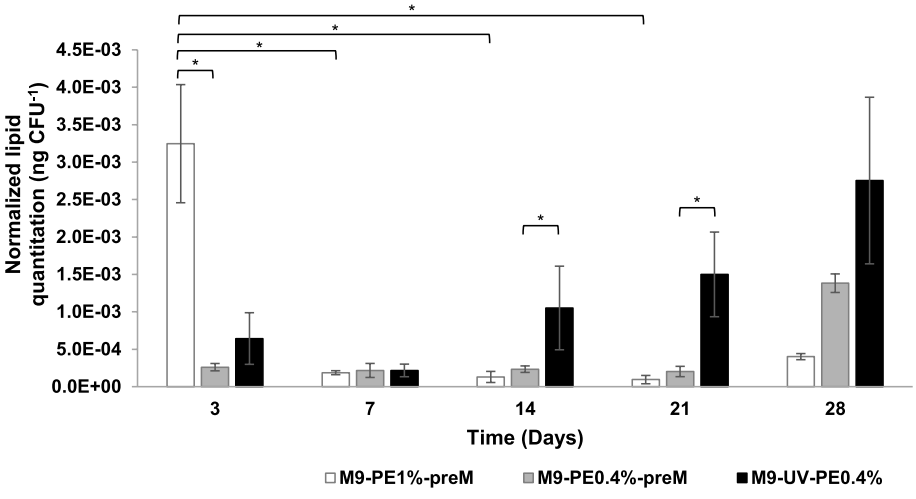


Fig. 3 Lipid accumulation of *R. opacus* R7 cells grown on different conditions, M9-PE1%-preM (white), M9-PE0.4%-preM (grey), and M9-UV-PE0.4% (black) obtained by sulfophosphovanillin (SPV) method. The lipid concentration value (mg CFU^{-1}) is presented as the mean value of two replicates ± Dev. St. The statistical significance was calculated by ANOVA followed by Tukey-adjusted post-hoc comparisons: *p*-value < 0.05 (*)

conditions ($p\text{-}value < 0.05$). At 3 days, lipid accumulation was significantly higher in M9-PE1%-preM than in M9-PE0.4%-preM ($p\text{-}value < 0.05$). At later time points, M9-UV-PE0.4% lipid accumulation was higher than M9-PE1%-preM at 14 days ($p\text{-}value < 0.05$) and 21 days ($p\text{-}value < 0.05$), whereas no significant differences among culture conditions were observed at 7 and 28 days.

M9-PE1%-preM showed a significant decrease of cell-associated lipid after 3 days and remained lower thereafter, with values at 7, 14, and 21 days significantly lower than those observed at 3 days ($p\text{-}value < 0.05$). This decrease in lipid quantity likely reflects the utilization of storage compounds under limited substrate availability. Although temporal changes within each condition evidenced that M9-PE0.4%-preM and M9-UV-PE0.4% did not show statistically significant changes over time, the increase of lipid values could suggest renewed lipid accumulation associated with prolonged metabolic stress and declining cell viability.

Intracellular lipid accumulation was evaluated in *R. opacus* R7 grown on malate as the only carbon and energy source (reference condition) up to exponential (8 h) or stationary (24 h) phases (Additional file 5—Figure S3). Despite lipid content increased during the stationary phase, as expected for reserve compound synthesis under nutrient limitation, the overall increase of accumulation remained limited. This profile represents a baseline metabolic reference, indicating that in the presence of an easily assimilable carbon source, *R. opacus* R7 maintains a balance between growth and lipid storage with limited modulation of lipid synthesis.

Fluorescence microscopy analyses were consistent with the quantitative lipid data (Additional file 6—Figure S4). DAPI staining revealed DNA-containing bacterial cells associated with LDPE, while Nile Red staining highlighted intracellular lipid inclusions. Cell viability was assessed independently by viable cell counting performed on the same cell aliquots.

In cultures grown with 1% PE at fixed concentration, Nile Red fluorescence was already evident in DAPI-positive cells at earlier growth stages (7 days), indicating an early lipid accumulation. In malate-grown cells, lipid accumulation was minimal during exponential growth and increased during the stationary phase. A similar pattern was observed in the PE 0.4% fed-batch condition, where lipid accumulation was higher in stationary-phase cells.

Microscopic observations closely mirrored SPV assay results in describing lipid accumulation dynamics in *R. opacus* R7 grown on LDPE. Based on the overall physiological profile, including lipid accumulation dynamics and viability trends, the M9-UV-PE0.4% condition was not selected for subsequent targeted analyses.

Assessment of DCM-extracted compounds associated with untreated LDPE attack by *Rhodococcus opacus* R7 by GC–MS analyses

The PE attack by *R. opacus* R7 grown in the presence of LDPE supplied either at 0.4% in fed-batch mode or at 1% PE was recorded at 0, 14, and 28 days by evaluating the compounds extracted with DCM by GC–MS analyses. The resulting chromatographic profiles were compared to those obtained on untreated LDPE powder not exposed to any (a)biotic degradation (no inoculum) (Additional file 7—Figure S5). A cell-only control, consisting of *R. opacus* R7 grown on malate (absence of PE), was also evaluated showing compounds associated with bacterial biomass, cellular lipids, or membrane components (Additional file 8—Table S3).

At the initial time point, the chromatographic profile was dominated by ketones and alkanes with carbon chain lengths mainly ranging between C12 and C25, and carboxylic acids with 16 and 25 carbon atoms (Fig. 4 and

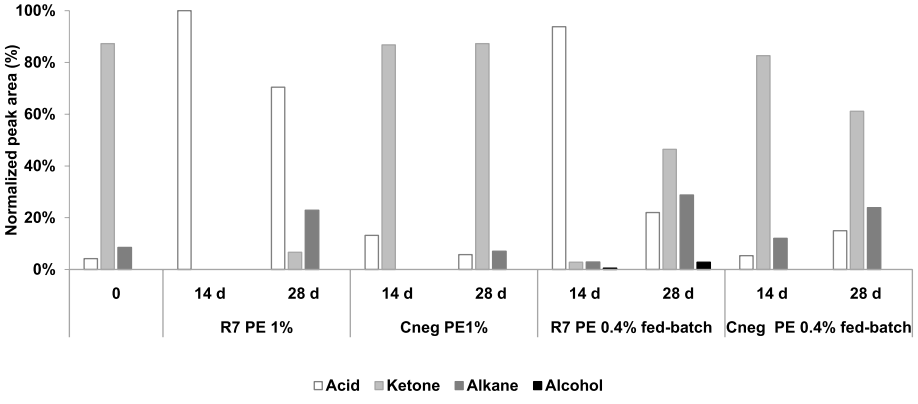


Fig. 4 Percentage of normalized peak area of product types deriving from *R. opacus* R7 growth on LDPE under two different conditions (R7 PE 1% corresponds to M9-PE1%-preM, R7 PE 0.4% fed-batch corresponds to M9-PE0.4%-preM) compared with the negative control (no inoculum) analyzed at 0, 14, and 28 days by GC-MSD analysis. The main product species after PE oxidation were carboxylic acids (white), ketones (light grey), alkanes (dark grey), and alcohols (black)

Table 1). These compounds likely reflect the background chemical profile of the commercial LDPE, which may include pre-existing oxidation products, low-molecular-weight PE fractions, or residual compounds associated with polymer manufacturing and handling. Since all samples were processed using the same extraction and derivatization procedures, and abiotic controls were included for comparison, subsequent changes in product distribution over time were interpreted relative to this initial/background profile.

During the incubation period, a change in relative abundance of ketones-carboxylic acids pattern was observed in both experimental conditions, whereas no substantial changes were detected in abiotic controls. Thus, the results showed changes in the relative distribution of DCM-extractable compounds including PE oxidation products during the entire incubation period in both settings with respect to abiotic controls.

In R7 cultures supplied with 1% PE (M9-PE1%-preM), a change of carboxylic acid species was detected at 14 days and 28 days, together with a relative higher number of long-chain acids and *n*-alkanes (C10-C21). On the other hand, under the 0.4% fed-batch condition (M9-PE0.4%-preM), the chemical profile was more heterogeneous with the simultaneous presence of ketones, alkanes, alcohols, and carboxylic acids at all time points. At 28 days, the fed-batch condition showed the appearance of several long-chain *n*-alkanes (C13-C29) that were not detected at the initial time point or in the corresponding abiotic controls.

The mode of PE supply strongly influenced the distribution of DCM-extractable compounds. The fixed 1% LDPE condition resulted in changes in the PE-associated extractable profile including oxidized compounds, whereas the fed-batch strategy promoted the coexistence of multiple intermediate classes, consistent with a continuous and asynchronous microbiologically influenced transformation of the polymer.

Rhodococcus opacus R7 gene selection and expression analyses upon growth on untreated LDPE

Target genes were selected based on previous transcriptomic data, literature evidence, and their potential involvement in PE degradation. Transcriptomic analyses of *R. opacus* R7 grown on LDPE revealed the up-regulation of genes encoding laccase-like multicopper oxidases (*LMCOs*), oxygenases such as 1-alkane monooxygenase (*alkB*), and hydroxylases including benzoate dioxygenase (*benA*) [26].

Genome analysis of *R. opacus* R7 revealed the presence of seven *LMCO* genes. Comparative multiple-sequence alignment of the seven identified LMCOs (aa sequences) showed moderate sequence identity among several isoenzymes, indicating the presence of conserved regions alongside significant divergence. This suggests that the R7 LMCOs may have distinct although potentially complementary functional roles during PE oxidation (Additional file 9—Table S4). In silico analyses further indicated that *LMCOs* harbor signal peptides consistent with extracellular secretion pathways (mainly TAT/SPI or TAT/SPII), supporting their possible involvement in extracellular PE oxidation. To further address the potential functional relevance of these enzymes, the seven R7 LMCOs were compared with LMCOs/laccases previously associated with PE oxidation or polymer oxidation, as well as with structurally characterized bacterial and fungal laccases. This comparison showed that LMCO1, LMCO2, LMCO4, and LMCO6 shared relatively high amino acid identity with C208, approximately 50%, whereas LMCO3 showed approximately 70% identity with 3GDC. By contrast, LMCO5 and LMCO7 displayed lower identity values, approximately 30% and 40%, respectively, with 3ZDW. Moreover, the other selected genes of R7 included a 1-alkane monooxygenase (*alkB*), a cytochrome P450 hydroxylase (*P450II*), and a benzoate dioxygenase (*benA*).

Gene expression was quantified by RT-qPCR using RNA extracted from cultures grown on LDPE supplied either at 0.4% (fed-batch) or 1% (fixed concentration), derived from a single pre-inoculum on malate. Expression levels were calculated using the ΔΔCt method, with malate-grown cells as the reference condition and 16S rRNA as the housekeeping gene.

The growth under the fed-batch PE 0.4% (M9-PE0.4%-preM) condition resulted in a broader and earlier activation of oxidative gene products, highlighting a more dynamic and coordinated transcriptional response. Indeed, at 3 days results show simultaneous expression of multiple *LMCOs* (*LMCO1*, *LMCO2*, *LMCO3*, *LMCO4*, *LMCO5*), *alkB*, *benA*, and *P450II*, indicating an early and coordinated gene activation (Fig. 5A). Notably, *LMCO2* and *LMCO3* evidenced particularly high expression at 3 days, suggesting a prominent role in the initial oxidation of the polymer. At 7 days, the expression profile shifted, with *LMCO1* becoming highly expressed, while *LMCO2* and *LMCO3* were no longer induced, and *alkB* and *benA* remained strongly expressed, consistent with ongoing metabolism of aliphatic and oxidized fragments. Additional induction of *LMCO4, LMCO5,* and *LMCO7* were recorded further suggesting the potential influence of substrate feeding strategy on the timing and specificity of *LMCO* gene activation.

The growth under the PE 1% (M9-PE1%-preM) condition showed the expression of several laccase-like multicopper oxidase genes (*LMCO1, LMCO2, LMCO3,* and *LMCO5*) at 3 days, supporting their role for extracellular or periplasmic oxidative systems during early LDPE oxidation. At 3 and 7 days the expression of *P450II* and

Table 1 Metabolic products detected by GC–MS analyses deriving from untreated commercial LDPE biodegradation by *R. opacus* R7 grown on LDPE in different conditions

Number	Compound[a]	Retention time (t_R) (min)	Molecular Weight	Formula	CAS Number	t0	R7 PE 1%		PE 1% - No inoculum		R7 PE 0.4% fed-batch		PE 0.4% fed-batch—No inoculum	
							14 d[b]	28d	14 d	28 d	14 d	28 d	14 d	28 d
1	2-Decanol, TMS derivative[c]	13.8	230.5	C13H30OSi	C13H30OSi	-	-	-	-	-	+[d]	-	-	-
2	Decanoic acid, TBDMS derivative	14.5	286.5	C16H34O2Si	104,255–74-5	-	+	+	-	-	-	+	-	-
3	Nonanoic acid, TMS derivative	15	230.4	C12H26O2Si	82,326–11-2	-	+	-	-	-	-	-	-	-
4	2-Dodecanone	15.6	184.2	C12H24O	6175–49-1	+	-	-	-	+	-	-	-	+
5	Tridecane, 7-hexyl-	15.62	268.5	C19H40	7225–66-3		-	-	-	-	-	+	-	-
6	Decanoic acid, TMS derivative	16.3	244.4	C13H28O2Si	55,494–15-0	-	-	+	-	-	-	-	+	
7	1-Tridecanol, TMS derivative	16.8	272.5	C16H36OSi	6009–33-2	-	-	-	-	-	-	+	-	-
8	Dodecanoic acid, TBDMS derivative	16.85	314.6	C18H38O2Si	104,255–77-8	-	-	+	-	-	+	-	-	-
9	Pentadecane	16.9	212.4	C15H32	629–62-9	+	-	-	-	+	-	-	-	+
10	Tetradecane, 3-methyl-	17.4	212.4	C15H32	18,435–22-8	-	-	-	-	-	-	+	-	-
11	Tetradecane, 4-ethyl-	17.968	226.4	C16H34	55,045–14-2	-	-	-	-	-	-	+	-	-
12	Tridecane, 7-hexyl-	18.057	268.5	C19H40	7225–66-3	-	-	-	-	-	-	+	-	-
13	5,5-Diethyltridecane	18.14	240.5	C17H36	17,453–92-8	-	-	+	-	-	+	+	-	-
14	2-Tetradecanone	18.2	212.4	C14H28O	2345–27-9	+	-	-	+	+	-	+	-	+
15	Dodecanoic acid, TMS ester	18.7	272.5	C15H32O2Si	55,520–95-1	-	-	+	-	-	-	+	-	+
16	Heptadecane	19.3	240.5	C17H36	629–78-7	+	-	-	-	+	-	-	+	+
17	5-Butyl-5-ethylheptadecane	19.7	324.6	C23H48	12,398 (CID)	-	-	-	-	-	-	+	-	-
18	Azelaic acid	20.3	188.2	C9H16O4	123–99-9	-	+	-	-	-	-	-	-	-
19	5,5-Diethylpentadecane	20.43	268.5	C19H40	85,977,274 (CID)	-	-	+	-	-	+	+	-	-
20	2-Hexadecanone	20.5	240.4	C16H32O	2345–28-0	+	-	-	+	+	-	-	+	+
21	Tetradecanoic acid, TMS derivative	20.9	300.5	C17H36O2Si	18,603–17-3	-	+	+	-	+	-	-	-	+
22	2-Pentadecanone, 6,10,14-trimethyl-	21.2	268.5	C18H36O	502–69-2	-	-	+	-	-	+	+	-	-
23	*n*-Pentadecanoic acid, TMS derivative	21.9	314.6	C18H38O2Si	74,367–22-9	-	+	+	-	-	-	-	-	-
24	Methyl *n*-hexadecyl ketone	22.5	268.5	C18H36O	7373–13-9	+	-	-	+	+	-	+	-	-
25	Hexadecenoic acid, (Z)-, TMS derivative	22.6	326.6	C19H38O2Si	5,352,900 (CID)	-	+	-	-	-	-	-	-	-
26	Hexadecanoic acid, TMS derivative	22.9	328.6	C19H40O2Si	55,520–89-3	+	+	+	+	+	+	+	-	-
27	Nonadecane	23.46	268.5	C19H40	629–92-5	+	-	+	-	+	+	+	+	+
28	10-Heptadecenoic acid, (Z)-, TMS derivative	23.6	340.6	C17H32O2	29,743–97-3		+		-	-	-		-	-
29	2-Nonadecanone	24.45	282.5	C19H38O	629–66-3	+		-	+	+	+	-	+	
30	9,12-Octadecadienoic acid (Z,Z)-, TMS derivative	24.46	352.6	C21H40O	56,259–07-5	-	+	-	-	-	-	-	-	+
31	Oleic Acid, (Z)-, TMS derivative	24.5	354.3	C21H42O2Si	21,556–26-3	-	+	-	-	-	-	-	-	-
32	trans-13-Octadecenoic acid, TMS derivative	24.55	354.6	C21H42O2Si	91,696,440 (CID)	-	+	-	-	-	-	-	-	-
33	Stearic acid, TMS derivative	24.7	356.6	C21H44O2Si	018748–91-9	+	+	+	+	+	+	+	-	+
34	Eicosane	25.2	282.5	C20H42	112–95-8	-	-	+	-	+	-	+	-	-
35	Heneicosane	25.7	296.6	C21H44	629–94-7	-	-	+	-	-	+	+	-	+
36	2-Docosanone	26.2	324.6	C22H44O	77,327–11-8	+	-	-	+	+	-	+	-	-
37	Eicosanoic acid, TMS derivative	26.4	384.7	C23H48O2Si	55,530–70-6	-	+	-	-	-	-	-	-	-
38	Pentacosane	26.9	352.6	C25H52	629–99-2	+	-	-	-	-	-	+	-	-
39	2-Pentacosanone	27.9	366.7	C25H50O	75,207–54-4	+	-	-	+	+	-	+	+	-
40	Heptacosane	28.6	380.7	C27H56	593–49-7	-	-	-	-	-	-	+	-	-

Table 1 (continued)

Number	Compound[a]	Retention time (t_R) (min)	Molecular Weight	Formula	CAS Number	t0	R7 PE 1%		PE 1% - No inoculum		R7 PE 0.4% fed-batch		PE 0.4% fed-batch—No inoculum	
							14 d[b]	28d	14 d	28 d	14 d	28 d	14 d	28 d
41	1,4-Benzenedicarboxylic acid, bis(2-ethylhexyl) ester	28.983	390.6	C24H38O4	6422–86-2		-	+	-	-	+	+	-	-
42	Nonacosane	30.7	408.7	C29H60	630–03–5	-	-	-	-	-	-	+	-	-

[a]Compound, the considered degradation products had more than 90% similarity compared with the mass spectra of NIST11

[b]14 d, number of days of incubation

[c]TMS derivative, trimethylsilyl derivative

[d]+, the symbol "+" indicates the presence of the compound, while "-" indicates the absence

alkB was detected, indicating their involvement in the further oxidation of polymer. *LMCO6* showed a delayed induction at 14 days, suggesting a role in later stages of the process, possibly related to the transformation of oxidized products (Fig. 5B).

These results indicate that LDPE attack by *R. opacus* R7 is a dynamic, multiphasic process, in which substrate availability and mode of supply modulate both the magnitude and temporal coordination of oxidative gene expression.

Induction of *Rhodococcus opacus* R7 genes in the presence of long-chain alkanes

Since medium and long-chain alkanes were dominant among the products observed by the GC–MS analysis (Fig. 4) and *R. opacus* R7 capability to grow on these substrates as the only carbon and energy source (Additional file 10—Figure S6) [29], we evaluated the expression of selected genes upon growth on two *n*-alkanes, tetracosane (C24; 0.1%) and hexatriacontane (C36; 0.8%) (Fig. 6). The growth assessment in the presence of long-chain alkanes could be a key point to investigate weather these compounds are potential inducers of PE-degrading enzymes.

Considering C24 growth, gene expression analyses revealed that *alkB* was highly expressed (31-fold), consistent with its role in *n*-alkane oxidation, and several *LMCO* genes (*LMCO2*, *LMCO5*, and *LMCO7*) showed strong induction (respectively, 19-fold, ninefold, and sixfold). This indicates that C24 efficiently induced a broad and coordinated oxidative response, supporting the idea that it can be an inducer for PE-oxidizing enzymes.

Although C36 supported growth of *R. opacus* R7, it induced the transcription of only a few genes with a low activation of the selected genes except for *LMCO6* (twofold). This induction likely reflects lower substrate bioavailability and slower cell activation.

These findings indicate that medium and long-chain *n*-alkanes, particularly C24, are effective inducers of genes associated with PE oxidation.

Discussion

Despite the rapid expansion of research on microbial plastic degradation, the field is increasingly moving beyond a sole emphasis on polymer depolymerization to prioritize the controlled production of value-added oxidized intermediates. This underscores the need for experimental frameworks that integrate different factors and scenarios [7, 10]. Polyethylene (PE) biodegradation remains a major scientific and technological challenge due to the chemical stability and high hydrophobicity of the polymer, which limit both enzymatic susceptibility and microbial colonization [9].

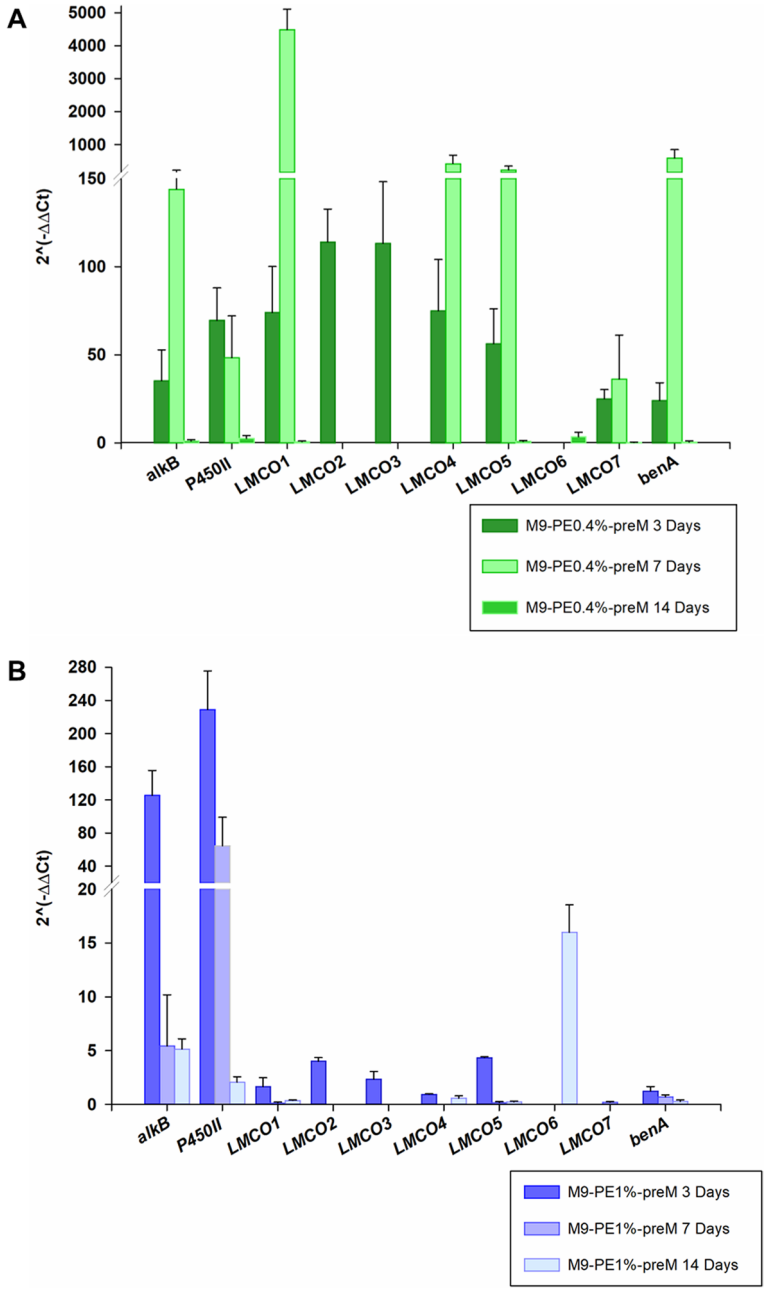


Fig. 5 Expression levels of *R. opacus* R7 selected genes encoding laccase-like multicopper oxidases (*LMCO1*, *LMCO2*, *LMCO3*, *LMCO4*, *LMCO5*, *LMCO6*, and *LMCO7*), 1-alkane monooxygenase (*alkB*), cytochrome P450 hydroxylase (*P450II*), and benzoate dioxygenase (*benA*). RT-qPCR experiments were conducted on cDNA deriving form RNA extracted from M9-PE1%-preM (**A**), or M9-PE0.4%-preM (**B**) at 3, 7, and 14 days. Expression levels were calculated relative to the malate-grown reference condition and normalized using 16S rRNA as the reference gene using the $2^{-\Delta\Delta Ct}$ method. Data are expressed as mean values of three replicates ± St. Dev

In this context, building on our previous transcriptomic characterization of *R. opacus* R7 grown on polyethylene (LDPE) [8, 26], the present study provides an integrated assessment of physiological, biochemical and transcriptional perspectives on PE attack under different cultivation strategies, including the combination of long-term growth experiments with enzymatic assays, lipid profiling, detection of oxidized products, and gene expression. This approach highlights the metabolic response of the strain to LDPE to be interpreted beyond simple growth or polymer alteration, offering insights into how cultivation strategy and substrate availability shape the trajectory of PE oxidation.

For growth experiments, the novelty was the extension of previous observations that *R. opacus* R7 can utilize LDPE as the sole carbon and energy source, sustaining

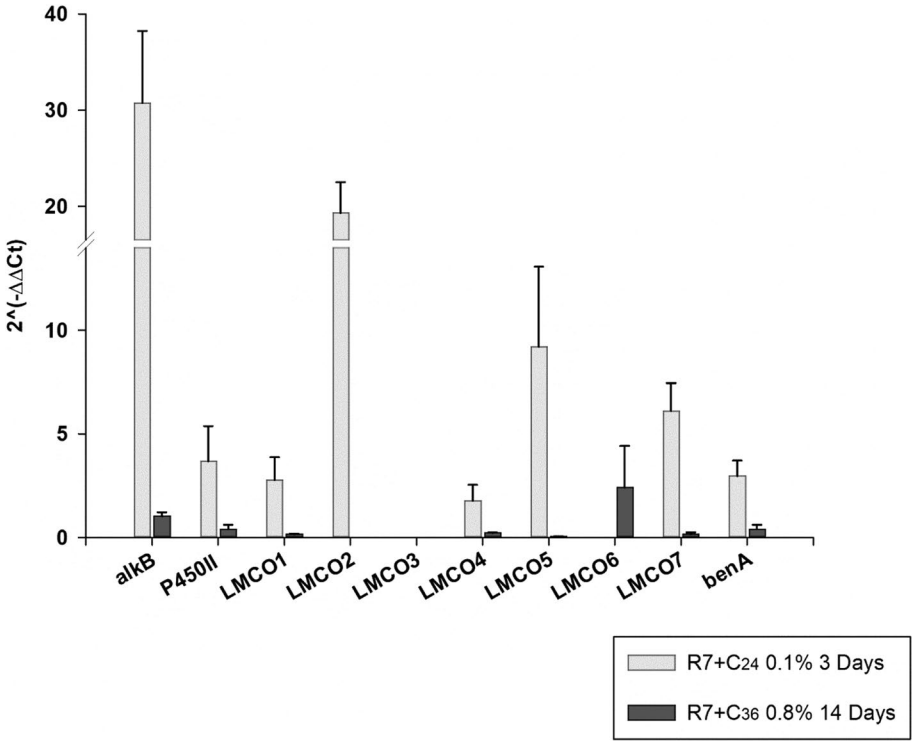


Fig. 6 Gene expression of *R. opacus* R7 grown on tetracosane (C24, 0.1%, sampled after 3 days; light grey) or hexatriacontane (C36, 0.8%, sampled after 14 days; dark grey) by RT-qPCR analyses. Expression levels were calculated relative to the malate-grown reference condition and normalized using 16S rRNA as the reference gene using the $2^{-\Delta\Delta Ct}$ method. Selected genes include laccase-like multicopper oxidases (*LMCO1*, *LMCO2*, *LMCO3*, *LMCO4*, *LMCO5*, *LMCO6*, and *LMCO7*), 1-alkane monooxygenase (*alkB*), cytochrome P450 hydroxylase (*P450II*), and benzoate dioxygenase (*benA*). Data are expressed as mean values of three biological replicates ± St. Dev

long-term growth up to 28 days [26]. Moreover, our data clearly show that growth performance is not solely determined by LDPE availability, but is strongly influenced by how the polymer is supplied and by the physiological state of the inoculum. Although fed-batch addition of LDPE at low concentration initially supported higher viable cell numbers compared to a single, high-dose LDPE addition, the cell number reach a similar value at later time points, suggesting that gradual substrate exposure reduces metabolic stress and improves colonization efficiency. It should be noted that the single-dose and repeated-supplementation conditions differ in both PE delivery schedule and cumulative PE input. Therefore, the observed differences cannot be attributed exclusively to the feeding mode, especially from 14 days. Instead, they should be interpreted as the outcome of distinct PE availability regimes.

Similar observations have been reported in hydrocarbon-degrading systems, where controlled substrate delivery prevents inhibitory effects associated with limited bioavailability or accumulation of poorly assimilable intermediates [17, 23].

Extracellular laccase activity was detected under all PE-growth conditions, corroborating previous reports on the involvement of laccase-like multicopper oxidases (LMCOs) in the initial oxidation of polyolefins [22, 25, 26]. However, laccase activity levels were only modestly affected by PE concentration, feeding strategy, or UV pretreatment and were linked to the physiological state of the inoculum (although with no statistical significance). Cultures derived from malate pre-inocula consistently showed higher laccase activity, in agreement with studies suggesting that metabolically active cells are more efficient at initiating extracellular oxidative processes [28]. Notably, UV pretreatment of PE did not enhance early laccase activity despite improving early growth, indicating that increased polymer accessibility does not directly translate into stronger laccase induction. Similar discrepancies have been reported in other studies, where abiotic pretreatments enhanced microbial colonization and growth but did not proportionally increase specific oxidative enzymatic activities [18]. Indeed, the UV-pretreated PE is a different substrate showing a hydrophilic surface with unsaturation and even ester bonds in the carbon chain. These factors underpin that laccases represent only one component of a broader oxidative network involved in PE transformation. Indeed, we hypothesized other enzymatic activities, such as lipase activity in the early kinetic times for UV-pretreated PE, as observed by Tao et al. [25].

Intracellular lipid accumulation emerged as a sensitive indicator of changes in the physiological state of *R. opacus* R7 during growth on LDPE. Lipid accumulation patterns differed markedly between cultivation strategies, with early lipid storage observed under fixed 1% PE conditions, whereas fed-batch PE resulted in delayed accumulation mainly during late growth stages. In oleaginous bacteria such as *Rhodococcus*, lipid accumulation is commonly associated with carbon excess, nutrient limitation, or metabolic imbalance [38, 39]. During LDPE growth, our data suggest that early lipid accumulation may reflect a stress-adaptive response or metabolically imbalanced state rather than efficient carbon assimilation alone. However, since no direct physiological stress markers were assessed in this study, this interpretation should be considered indicative and not conclusive. The observation that UV-oxidized LDPE increased late-stage lipid accumulation growth arrest and further suggests that lipid storage is unlikely to be the primary driver without preventing of growth limitation. These findings suggest that additional factors, such as depletion of accessible polymer fractions, persistence of crystalline PE regions, or accumulation of poorly assimilable intermediates, may also contribute to the observed growth plateau. Comparable conclusions have been drawn in studies on *R. ruber* and *R. erythropolis*, where lipid accumulation accompanied stress conditions or incomplete substrate utilization rather than enhanced degradation efficiency [23, 40, 41].

GC–MS product analysis provided direct chemical evidence of LDPE attack, revealing dynamic shifts in the composition of extracted products over time. The decrease in ketone types and the detection of novel carboxylic acids in biotic samples compared to abiotic controls are consistent with oxidation of the polymer, as previously reported for PE-degrading *Rhodococcus* spp. [23–25]. Importantly, the feeding strategy influenced the distribution of observed products: the fixed 1% PE condition favored the presence of oxidized compounds such as carboxylic acids, whereas the fed-batch strategy resulted in a heterogeneous mixture of alkanes, alcohols, ketones, and acids. At final time-point, the occurrence of medium- and long-chain alkanes and fatty acids supports the notion that PE attack proceeds through partial oxidation and a possible fragmentation. Therefore, this supports the hypothesis that fed-batch PE promotes continuous and asynchronous polymer transformation, preventing the presence of single product classes and potentially reducing feedback inhibition. Similar product heterogeneity has been described in systems where PE degradation proceeds via multiple, partially overlapping oxidative pathways rather than a single linear route [30].

Concerning the transcriptional analyses, they further highlighted the multiphasic and adaptive nature of LDPE metabolism in *R. opacus* R7. These analyses were based on R7 selected target genes, including LMCOs that are closely related to previously described oxidative enzymes, while others may represent more divergent LMCOs with potentially distinct substrate specificities. Growth under fed-batch PE conditions triggered an early and coordinated expression of multiple oxidative enzymes, including several LMCOs, *alkB*, *benA*, and *P450II*. The fixed 1% PE condition induced a temporally segregated response, with early activation of *alkB* and *P450II* as well as *LMCO1*, *LMCO2, LMCO3*, and *LMCO5* genes, followed by delayed induction of specific *LMCOs* such as *LMCO6*. These novel findings extend previous transcriptomic studies on *R. opacus* R7 conducted at 3 days of growth on LDPE [26] and support the idea of functional specialization among LMCO enzymes, with distinct roles during different stages of polymer oxidation. Comparable temporal regulation of oxidative systems has been reported in other hydrocarbon-degrading bacteria, where early monooxygenases initiate substrate activation, and later enzymes process downstream intermediates [13, 14].

Finally, the experiments with long-chain *n*-alkanes further strengthen the link between hydrocarbon metabolism and LDPE attack. Tetracosane (C24) acted as a strong inducer of *alkB* and multiple *LMCO* genes. This observation aligns with previous studies showing that medium-chain alkanes are effective inducers of oxidative pathways involved in plastic and hydrocarbon degradation [12, 29, 42]. Hexatriacontane (C36) elicited a transcriptional responses of only LMCO6, likely due to lower bioavailability and slower uptake, despite supporting growth. These results emphasize that substrate accessibility and chain length are critical determinants of transcriptional induction and suggest that alkane-like PE fragments may act as key metabolic signals during polymer degradation.

Taken together, our results support a model in which PE attack by *R. opacus* R7 proceeds through a complex and multiphasic step. Multi-level and multi-omics approaches highlighted an oxidative network influenced by substrate availability and cultivation strategy, resulting in a mechanistic framework for improving microbial PE oxidation and advancing sustainable plastic waste biodegradation.

This study demonstrates that LDPE attack by *Rhodococcus opacus* R7 is a complex and multiphasic metabolic process shaped by substrate accessibility, cultivation strategy, and cell physiological state.

From a biotechnological perspective, these findings highlight the importance of process design, such as fed-batch strategies and the use of suitable inducers to steer PE transformation toward controlled oxidation and valorization rather than incomplete or stress-driven metabolism.

Supplementary Information

The online version contains supplementary material available at https://doi.org/10.1186/s12866-026-05315-x.

Additional file 1: Table S1. List of *Rhodococcus* sp. strains able to oxidize and/or biotransform different types of PE [8, 22–24, 26, 28, 43–45].

Additional file 2: Table S2. List of primers for RT-qPCR experiments [26].

Additional file 3: Fig. S1. Growth kinetic curves of *R. opacus* R7 measured by optical density at 600 nm (OD_{600}) and viable cell counts (CFU mL^{-1}) under different conditions: (A) M9-PE1%, (B) M9-PE0.4%, (C) M9-PE1%-preM, (D) M9-PE0.4%-preM, and (E) M9-UV-PE0.4%. The growth values are represented as mean ± st. dev.

Additional file 4: Fig. S2. Relative lipase activity (U mL^{-1}) of the supernatants (CFS) of *R. opacus* R7 grown on UV-pretreated LDPE administered in a fed-batch mode at 0.4% PE. The hydrolytic activity is reported as the mean of three replicates ± SE.

Additional file 5: Fig. S3. Lipid accumulation of *R. opacus* R7 cells grown on 20 mM malate up to 8 h or 24 h obtained by SPV method. The lipid concentration value (mg CFU^{-1}) is presented as the mean value of two replicates ± St. Dev.

Additional file 6: Fig. S4. Lipid accumulation of *R. opacus* R7 using fluorescence microscopy comparing different growth phases and conditions. Scale bar 5 µm.

Additional file 7: Fig. S5. Chromatogram profiles by GC-MS analyses of the following derivatized DCM extracts: commercial LDPE powder in M9 mineral medium at initial time (A), *R. opacus* R7 grown on fed-batch PE 0.4% at 14 days (B), and 28 days (D), the condition without inoculum at 14 days (C), and 28 days (E), *R. opacus* R7 grown on PE 1% at 14 days (F), and 28 days (H), the condition without inoculum at 14 days (G), and 28 days (I).

Additional file 8: Table S3. Metabolic products detected by GC-MS analyses deriving from *R. opacus* R7 grown on malate 20 mM (M9-M) at 24 h.

Additional file 9: Table S4.*R. opacus* R7 LMCO amino acid sequence identity expressed in percentage obtained by Clustal Omega multiple sequence alignment (MSA) tool with the default settings.

Additional file 10: Fig. S6. Time required by *R. opacus* R7 to reach the exponential phase (OD_{600} = 0.8) using medium- and long-chain *n*-alkanes with 24 (C24) or 36 (C36) carbon atoms as the sole carbon and energy sources.

Authors' contributions

Author contributions JZ: Conceptualization, Data curation, Investigation, Methodology, Software, Validation, Visualization, Writing – original draft and review & editing. MS: Methodology, Data curation, Writing – original draft and review & editing. VV: Data curation, Methodology, Software, Visualization. ML: Funding acquisition, Project administration, Resources. PDG: Conceptualization, Funding acquisition, Project administration, Resources, Supervision, Writing—review & editing. All authors contributed to the article and approved the submitted version.

Funding

This work was funded by 2024-ATE-0471 from University of Milano-Bicocca.

Data availability

The authors confirm that the data supporting the findings of the study are available within the article and the supplementary files.

Declarations

Ethics approval and consent to participate

Not applicable.

Consent for publication

Not applicable.

Competing interests

The authors declare no competing interests.

Author details

[1]Department of Biotechnology and Biosciences, University of Milano-Bicocca, Piazza Della Scienza, 2, Milan 20126, Italy
[2]Department of Earth and Environmental Sciences, University of Milano-Bicocca, Piazza Della Scienza, 1, Milan 20126, Italy

Received: 17 April 2026 / Accepted: 15 June 2026
Published online: 04 July 2026

References

1. Mufarrij F, Ashrafi O, Navarri P, Khojasteh Y. Development and lifecycle assessment of various low- and high-density polyethylene production processes based on CO_2 capture and utilization. J Clean Prod. 2023;414:137624. https://doi.org/10.1016/j.jclepro.2023.137624.
2. PlasticsEurope. Plastics – The Fast Facts. Plastics Europe AISBL 2024. https://plasticseurope.org/knowledge-hub/plastics-the-fast-facts-2024/. Accessed 2 Febr 2026.
3. Sen SK, Raut S. Microbial degradation of low density polyethylene (LDPE): a review. J Environ Chem Eng. 2015;3:462–73. https://doi.org/10.1016/j.jece.2015.01.003.
4. Mohanan N, Montazer Z, Sharma PK, Levin DB. Microbial and enzymatic degradation of synthetic plastics. Front Microbiol. 2020;11:580709. https://doi.org/10.3389/fmicb.2020.580709.
5. OECD. Distribution of plastic waste management worldwide in 2019, by region and method [Graph]. Statista. 2022. https://www.statista.com/statistics/1358376/global-plastic-waste-management-share-by-region/. Accessed 17 Sept 2025.
6. Ellis LD, Rorrer NA, Sullivan KP, Otto M, McGeehan JE, Román-Leshkov Y, et al. Chemical and biological catalysis for plastics recycling and upcycling. Nat Catal. 2021;4:539–56. https://doi.org/10.1038/s41929-021-00648-4.
7. Andler R, Tiso T, Blank L, Andreeßen C, Zampolli J, D'Afonseca V, et al. Current progress on the biodegradation of synthetic plastics: from fundamentals to biotechnological applications. Rev Environ Sci Biotechnol. 2022;21:829–50. https://doi.org/10.1007/s11157-022-09631-2.
8. Zampolli J, Collina E, Lasagni M, Di Gennaro P. Insights into polyethylene biodegradative fingerprint of *Pseudomonas citronellolis* E5 and *Rhodococcus erythropolis* D4 by phenotypic and genome-based comparative analyses. Front Bioeng Biotechnol. 2024;12:1472309. https://doi.org/10.3389/fbioe.2024.1472309.
9. Pérez-García P, Sass K, Wongwattanarat S, Amann J, Feuerriegel G, Neumann T, et al. Microbial plastic degradation: enzymes, pathways, challenges, and perspectives. Microbiol Mol Biol Rev. 2025;89:e00087-e124. https://doi.org/10.1128/mmbr.00087-24.
10. Purohit A, Cochereau B, Sarkar O, Rova U, Christakopoulos P, Antonopoulou I, et al. Polyethylene biodegradation: a multifaceted approach. Biotechnol Adv. 2025;82:108577. https://doi.org/10.1016/j.biotechadv.2025.108577.
11. Yoon MG, Jeon JH, Kim MN. Biodegradation of polyethylene by a soil bacterium and AlkB cloned recombinant cell. J Bioremed Biodegrad. 2012;3:145. https://doi.org/10.4172/2155-6199.1000145.
12. Suzuki M, Hayashi T, Takahashi K, Nozaki K, Kasuya K. Exploring biodegradation limits of n-alkanes as polyethylene models using multi-omics approaches. Sci Total Environ. 2025;977:179365. https://doi.org/10.1016/j.scitotenv.2025.179365.
13. Rojo F. Degradation of alkanes by bacteria. Environ Microbiol. 2009;11:2477–90. https://doi.org/10.1111/j.1462-2920.2009.01948.x.
14. Cappelletti M, Fedi S, Frascari D, Ohtake H, Turner RJ, Zannoni D. Analyses of both the *alkB* gene transcriptional start site and *alkB* promoter-inducing properties of *Rhodococcus* sp. strain BCP1 grown on n-alkanes. Appl Environ Microbiol. 2011;77:1619–27. https://doi.org/10.1128/AEM.01987-10.
15. Taxeidis G, Nikolaivits E, Siaperas R, Gkountela C, Vouyiouka S, Pantelic B, et al. Triggering and identifying the polyurethane and polyethylene-degrading machinery of filamentous fungi secretomes. Environ Pollut. 2023;325:121460. https://doi.org/10.1016/j.envpol.2023.121460.
16. Siaperas R, Taxeidis G, Gioti A, Nikolaivits E, Topakas E. Multi-omics insights into the response of *Aspergillus parasiticus* to long-chain alkanes in relation to polyethylene modification. Environ Pollut. 2025;376:126386. https://doi.org/10.1016/j.envpol.2025.126386.

17. Soleimani Z, Gharavi S, Soudi M, Moosavi-Nejad Z. A survey of intact low-density polyethylene film biodegradation by terrestrial Actinobacterial species. Int Microbiol. 2021;24:65–73. https://doi.org/10.1007/s10123-020-00142-0.
18. Liu L, Zhang M, Xu H, Blažević Z, Ballerstedt H, Blank LM. Challenges of polyethylene (PE) biodegradation – a perspective. Biotechnol Adv. 2025;85:108717. https://doi.org/10.1016/j.biotechadv.2025.108717.
19. Kong Y, Wang R, Zhou Q, Li J, Fan Y, Chen Q. Recent progresses and perspectives of polyethylene biodegradation by bacteria and fungi: a review. J Contam Hydrol. 2025;269:104499. https://doi.org/10.1016/j.jconhyd.2025.104499.
20. Zampolli J, Zeaiter Z, Di Canito A, Di Gennaro P. Genome analysis and -omics approaches provide new insights into the biodegradation potential of *Rhodococcus*. Appl Microbiol Biotechnol. 2019;103:1069–80. https://doi.org/10.1007/s00253-018-9539-7.
21. Zampolli J, Orro A, Vezzini D, Di Gennaro P. Genome-based exploration of *Rhodococcus* species for plastic-degrading genetic determinants using bioinformatic analysis. Microorganisms. 2022;10:1846. https://doi.org/10.3390/microorganisms10091846.
22. Santo M, Weitsman R, Sivan A. The role of the copper-binding enzyme-laccase - in the biodegradation of polyethylene by the actinomycete *Rhodococcus ruber*. Int Biodeterior Biodegrad. 2013;84:204–10. https://doi.org/10.1016/j.ibiod.2012.03.001.
23. Gravouil K, Ferru-Clement R, Colas S, Heyle R, Kadri L, Bourdeau L, et al. Transcriptomics and lipidomics of the environmental strain *Rhodococcus ruber* point out consumption pathways and potential metabolic bottlenecks for polyethylene degradation. Environ Sci Technol. 2017;51:5172–81. https://doi.org/10.1021/acs.est.7b00846.
24. Orr IG, Hadar Y, Sivan A. Colonization, biofilm formation and biodegradation of polyethylene by a strain of *Rhodococcus ruber*. Appl Microbiol Biotechnol. 2004;65:97–104. https://doi.org/10.1007/s00253-004-1584-8.
25. Tao X, Ouyang H, Zhou A, Wang D, Matlock H, Morgan JS. Polyethylene degradation by a *Rhodococcous* strain isolated from naturally weathered plastic waste enrichment. Environ Sci Technol. 2023;57:13901–11. https://doi.org/10.1021/acs.est.3c03778.
26. Zampolli J, Orro A, Manconi A, Ami D, Natalello A, Di Gennaro P. Transcriptomic analysis of *Rhodococcus opacus* R7 grown on polyethylene by RNA-seq. Sci Rep. 2021;11:21311. https://doi.org/10.1038/s41598-021-00525-x.
27. Zampolli J, Vezzini D, Brocca S, Di Gennaro P. Insights into the biodegradation of polycaprolactone through genomic analysis of two plastic-degrading *Rhodococcus* bacteria. Front Microbiol. 2024;14:1284956. https://doi.org/10.3389/fmicb.2023.1284956.
28. Zampolli J, Mangiagalli M, Vezzini D, Lasagni M, Ami D, Natalello A, et al. Oxidative degradation of polyethylene by two novel laccase-like multicopper oxidases from *Rhodococcus opacus* R7. Environ Technol Innov. 2023;32:103273. https://doi.org/10.1016/j.eti.2023.103273.
29. Zampolli J, Collina E, Lasagni M, Di Gennaro P. Biodegradation of variable-chain-length *n*-alkanes in *Rhodococcus opacus* R7 and the involvement of an alkane hydroxylase system in the metabolism. AMB Express. 2014;4:73. https://doi.org/10.1186/s13568-014-0073-4.
30. Jendrossek D. Polyethylene and related hydrocarbon polymers ("plastics") are not biodegradable. New Biotechnol. 2024;83:231–8. https://doi.org/10.1016/j.nbt.2024.08.503.
31. Hou L, Xi J, Liu J, Wang P, Xu T, Liu T, et al. Biodegradability of polyethylene mulching film by two *Pseudomonas* bacteria and their potential degradation mechanism. Chemosphere. 2022;286:131758. https://doi.org/10.1016/j.chemosphere.2021.131758.
32. Maniatis T, Fritsch EF, Sambrook J. Molecular cloning: a laboratory manual. New York: Cold Spring Harbor Laboratory; 1982.
33. Anschau A, Caruso CS, Kuhn RC, Franco TT. Validation of the sulfo-phospho-vanillin (SPV) method for the determination of lipid content in oleaginous microorganisms. Braz J Chem Eng. 2017;34:19–27. https://doi.org/10.1590/0104-6632.20170341s20140222.
34. Aziz RK, Bartels D, Best AA, DeJongh M, Disz T, Edwards RA, et al. The RAST server: rapid annotations using subsystems technology. BMC Genomics. 2008;9:75. https://doi.org/10.1186/1471-2164-9-75.
35. Altschul SF, Gish W, Miller W, Myers EW, Lipman DJ. Basic local alignment search tool. J Mol Biol. 1990;215:403–10. https://doi.org/10.1016/S0022-2836(05)80360-2.
36. Sievers F, Wilm A, Dineen D, Gibson TJ, Karplus K, Li W, et al. Fast, scalable generation of high-quality protein multiple sequence alignments using Clustal Omega. Mol Syst Biol. 2011;7:539. https://doi.org/10.1038/msb.2011.75.
37. Teufel F, Almagro Armenteros JJ, Johansen AR, Gíslason MH, Pihl SI, Tsirigos KD, et al. SignalP 6.0 predicts all five types of signal peptides using protein language models. Nat Biotechnol. 2022;40:1023–5. https://doi.org/10.1038/s41587-021-01156-3.
38. Alvarez HM, Silva RA, Herrero M, Hernández MA, Villalba MS. Metabolism of triacylglycerols in *Rhodococcus* species: insights from physiology and molecular genetics. J Mol Biochem. 2013;2:69–78 (**ISSN: 2241-0090**).
39. Alvarez HM, Herrero OM, Silva RA, Hernández MA, Lanfranconi MP, Villalba MS. Insights into the Metabolism of Oleaginous *Rhodococcus* spp. Appl Environ Microbiol. 2019;85:e00498-e519. https://doi.org/10.1128/AEM.00498-19.
40. de Carvalho CCCR, Marques MPC, Hachicho N, Heipieper HJ. Rapid adaptation of *Rhodococcus erythropolis* cells to salt stress by synthesizing polyunsaturated fatty acids. Appl Microbiol Biotechnol. 2014;98:5599–606. https://doi.org/10.1007/s00253-014-5549-2.
41. Yoshida N, Yano T, Kedo K, Takuya F, Nagai R, Iwano M, et al. A unique intracellular compartment formed during the oligotrophic growth of *Rhodococcus erythropolis* N9T–4. Appl Microbiol Biotechnol. 2017;101:331–40. https://doi.org/10.1007/s00253-016-7883-z.
42. Montazer Z, Najafi MBH, Levin DB. Challenges with verifying microbial degradation of polyethylene. Polymers. 2020;12:123. https://doi.org/10.3390/polym12010123.
43. Rong Z, Ding ZH, Wu YH, Xu XW. Degradation of low-density polyethylene by the bacterium *Rhodococcus* sp. C-2 isolated from seawater. Sci Total Environ. 2024;907:167993. https://doi.org/10.1016/j.scitotenv.2023.167993.
44. Eyheraguibel B, Traikia M, Fontanella S, Sancelme M, Bonhomme S, Fromageot D, et al. Characterization of oxidized oligomers from polyethylene films by mass spectrometry and NMR spectroscopy before and after biodegradation by a *Rhodococcus rhodochrous* strain. Chemosphere. 2017;184:366–74. https://doi.org/10.1016/j.chemosphere.2017.05.137.
45. Goudriaan M, Morales VH, van der Meer MT, Mets A, Ndhlovu RT, van Heerwaarden J, et al. A stable isotope assay with ^{13}C-labeled polyethylene to investigate plastic mineralization mediated by *Rhodococcus ruber*. Mar Pollut Bull. 2023;186:114369. https://doi.org/10.1016/j.marpolbul.2022.114369.

Publisher's Note

Springer Nature remains neutral with regard to jurisdictional claims in published maps and institutional affiliations.